Development of Shock Absorbing Barrier Materials for High Performance Magazine Construction

Claudio Herzfeld and Sean Wise
CEMCOM Research Associates

Abstract:

To prevent sympathetic detonation in a high performance magazine, barriers between stacks of munitions absorb donor fragments. Acceptor munitions may still initiate on impact of barrier debris or on being thrown into the walls of the magazine itself. These shocks can be reduced to a safe level by increasing the barrier's mass which reduces its velocity and the imparted shock. In addition a porous outer lining material shields the acceptors from the heavier barriers and the magazine's walls.

The acceleration forces on munitions during lining penetration are a function of the compressive strength and density of the lining and the mass, interaction area and velocity of the impacting munitions. The strength of the porous lining must be tailored so acceleration forces do not reach shock loading and yet providing sufficient deceleration so the thickness of the porous lining can be reduced. A high porosity in the lining is important, since the dynamic strength of the material will govern the impact loading until all the porosity is crushed out. Therefor high porosity at the optimum compressive strength will produce the most efficient lining system.

A porous light-weight inorganic material that satisfies these performance criteria has been successfully tested. This material will be compared to a new system under development. The new material's reduced cost allows large scale use in magazine construction. The new system can be pre-fabricated or placed by standard methods. The new lining is also being considered as a replacement for concrete in structural elements in the high performance magazine and general construction.

1. INTRODUCTION

The High Performance Magazine (HPM) is designed to increase the allowable net explosive weight (NEW) of munitions stored within a limited area by placing ordnance stacks in cells which are effectively shielded from one another with respect to sympathetic detonation. The maximum credible event from an unintended detonation is then limited to the NEW of the munitions in a given cell. Since propagation between stacks is often caused by impacting donor fragments on acceptors, walls placed between cells must provide ballistic protection against these very high speed chards of metal. The wall itself, however, can also become a hazard as it will impact acceptor stacks at a speed that is inversely proportional to its mass and directly proportional to the blast impulse from the donor explosive. Essentially, the wall must

Report Documentation Page

Form Approved
OMB No. 0704-0188

1. REPORT DATE **AUG 1994**	2. REPORT TYPE	3. DATES COVERED **00-00-1994 to 00-00-1994**

4. TITLE AND SUBTITLE **Development of Shock Absorbing Barrier Materials for High Performance Magazine Construction**	5a. CONTRACT NUMBER 5b. GRANT NUMBER 5c. PROGRAM ELEMENT NUMBER
6. AUTHOR(S)	5d. PROJECT NUMBER 5e. TASK NUMBER 5f. WORK UNIT NUMBER
7. PERFORMING ORGANIZATION NAME(S) AND ADDRESS(ES) **CEMCOM Research Associates,1919 Halethorpe farms Rd,Baltimore,MD,21227-4502**	8. PERFORMING ORGANIZATION REPORT NUMBER
9. SPONSORING/MONITORING AGENCY NAME(S) AND ADDRESS(ES)	10. SPONSOR/MONITOR’S ACRONYM(S) 11. SPONSOR/MONITOR’S REPORT NUMBER(S)

12. DISTRIBUTION/AVAILABILITY STATEMENT
Approved for public release; distribution unlimited

13. SUPPLEMENTARY NOTES
See also ADM000767. Proceedings of the Twenty-Sixth DoD Explosives Safety Seminar Held in Miami, FL on 16-18 August 1994.

14. ABSTRACT
see report

15. SUBJECT TERMS

16. SECURITY CLASSIFICATION OF:			17. LIMITATION OF ABSTRACT	18. NUMBER OF PAGES	19a. NAME OF RESPONSIBLE PERSON
a. REPORT **unclassified**	b. ABSTRACT **unclassified**	c. THIS PAGE **unclassified**	**Same as Report (SAR)**	**18**	

Standard Form 298 (Rev. 8-98)
Prescribed by ANSI Std Z39-18

intercept the very high velocity donor fragments while, at the same time, impart to the acceptors only soft, low stress impacts from the barrier's debris. These seemingly contradictory requirements can be accomodated because the deceleration stress on the high speed fragments is primarily a function of barrier density while the stress from lower velocity impacts of the debris on the acceptors is a function of the barrier's dyanmic mechanical strength. Thus, dense granular materials make effective fragment barriers.

Loose, uncompacted granular materials will impart very low stress to objects that are impacted. At higher speed, however, the particles compact and lock up so that they act more like a solid. This Hugoniot relationship in stress and particle velocity space is shown if Fig. 1 for a solid, polymethylmethacrylate (PMMA), a granular material (sand), and a high porosity shock absorbing chemically bonded ceramic (SA/CBC) material GC2. The stress on the acceptors is proportional to the velocity of the impact. The velocity can be reduced through an increase in the wall's mass or reducing the weight of the donor explosive in a single cell. Both these solutions lead to an inefficient use of the magazine's internal volume. But if a shock absorbing material is placed over the fragment barrier's surface, the stress of the wall debris striking the acceptors is made much less sentitive to velocity. Because of this, a barrier with a shock absorbing liner can be more space efficient. It will also provide a cushion for acceptors accelerated at the walls.

Fig. 1 Impact Hugoniot Curves

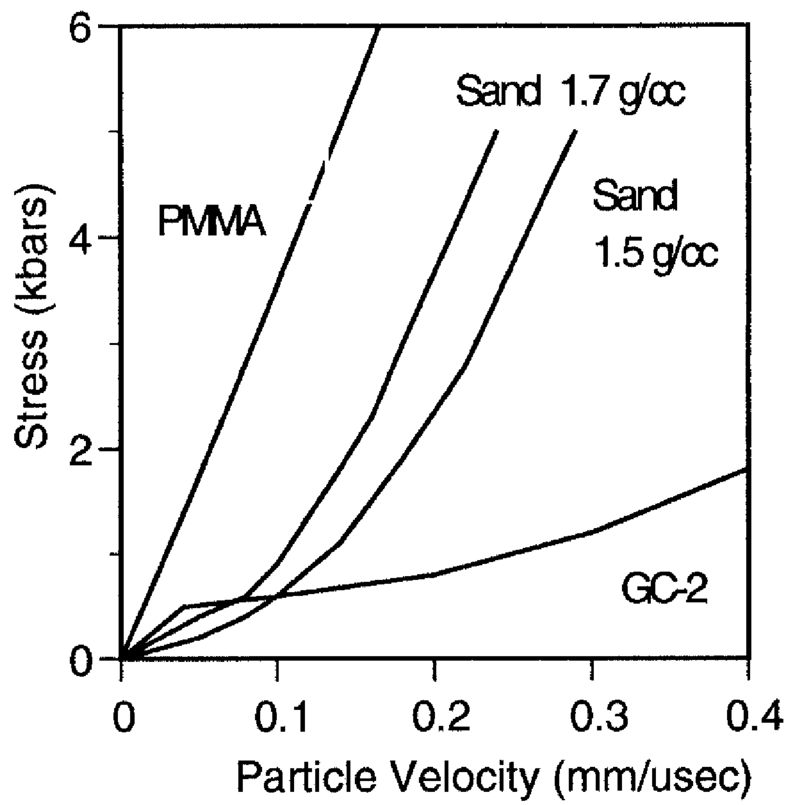

Fig. 1 Impact Hugoniot Curves

Experiments conducted by the Navy showed that inserting a heavy granular barrier material between panels of the highly porous SA/CBC material GC2 can reduce the acceleration on the acceptors by more than 10 fold. When a wall faced with the SA/CBC strikes an acceptor, the loading is limited to the elastic compressive yield stress until the CBC porosity is completely crushed out of the system. The acceleration on the acceptors will be a function of this yield stress so long as the acceptors strike the wall fast enough to exceed this stress, and the wall is thick enough such that the porosity is not completely lost. Volume efficiency of the shock absorbing layer will be proportional to its yield strength and its total pore volume. Very high pore volume is clearly desirable, but care must be taken to insure that the elastic yield stress stays within a range that leads to acceptable loading of the acceptors. If the minimum stress to crush the material is too high, the acceptors will receive too high an acceleration. On the other hand, if the stress is too low, the shock absorbing layer will "bottom out" if it is too thin or require more material so that the volume efficiency is lost.

Tests and analysis by the Naval Facilities Engineering Service Center NFESC on SA/CBC

GC2 showed that a material with static yield strength of 1500 to 2500 psi and porosity in excess of 60% should provide a good shock absorption layer for the walls. 12-18" of GC2 panel thickness is needed to provide a thick enough cushion to prevent bottoming out when impacted. The mechanical properties needed are in the range of lightweight concretes which can be used for low rise construction (up to 30 feet tall). The pore volume needed requires using a lightweight concrete with a density around 800 kg/m^3 (50 lb/ft^3). The GC2 material meets these requirements. But it was designed to be used in much smaller volume, and its cure sequence requires oven drying, so it is not a good candidate for manufacture of the large panels needed in the High Performance Magazine. The shock absorbing material used to line the non-propagating barriers in the HPM magazine needs to meet the strength and porosity characteristics listed above, but be less than \$200/yd^3, be capable of being formed on site and, since it could be used structurally, bond well to reinforcing elements, and have a low cure shrinkage. These targets are summarized in Table I.

Table I Target Properties for SA/CBC Materials

SA/CBC Materials	GC2	Target	**Units**
Comp. Strength	**8.3**	**10-17**	**MPa**
	1200	1500-2500	psi
Porosity	**75**	**>60**	**%**
Density	**550**	**<800**	**kg/m^3**
	35	<50	lbs/ft^3
Shrinkage	**0.22**	**<0.1**	**%**
Materials Costs	**920**	**<260**	**\$/m^3**
	700	<200	\$/yd^3
Manufacturing	Pre-fab	On Site or Pre-fab	
Bond to Rebar		yes	
Fire Resistance		yes	

Table I Target Properties for SA/CBC Materials

To meet these targets, Cemcom evaluated new cementitious formulations with different filler packages. The candidate materials use lower cost ingredients and the cure does not include an oven drying cycle like GC-2 to remove mixing water. Therefore it can be placed and cured like a regular concrete at a job site.

Once a formulation was obtained that had properties within the target range and its mixing and placing procedures were refined, it was labeled "MWB50". Samples of this formulation were submitted to Construction Technologies Laboratories (CTL) to be tested for their structural performance characteristics. These included standard test cylinders for strength and creep, freeze-thaw prisms, and intermediate scale reinforced structural elements designed to the American Concrete Institute's (ACI) Building Code Requirements for Reinforced Concrete. The mechanical evaluation of the materials at 28 days has been completed, but many of the long term tests are still in progress. This paper talks about the mix development, process development and structural characterization of the liner material for the high performance magazine's barrier walls.

2. MATERIALS DEVELOPMENT

The candidate material was developed by screening mix formulations prepared in a 12 quart planetary paddle mixer. Initial screening focused on obtaining the target porosity (as estimated from the density) coupled with an acceptable strength. Once acceptable physical properties were obtained, the preferred mixes were scaled up to a 1/3 yd^3 batch size in a 12 ft^3 horizontal mortar mixer. The characterization tests were repeated with larger samples sizes. Compressive strengths[1] and elastic moduli were measured on 4"x8" and 6"x12" cylinders. Splitting tensile strengths[2] were measured on 4"x4" and 6"x12" cylinders. Flexure properties were evaluated on 4"x6"x36" beams[3].

Cure Process Development

The samples were initially cured for 7 days in-mold at high humidity and then held at ambient temperature and humidity (Cure 1). Strengths were measured at 28 days while weight and length changes[4] were monitored at this time and at 3 months. The rate of drying and the drying shrinkage for cure 1 were found to be higher than desirable, so an extension of the moist cure to 28 days was examined (Cure 2). These samples remained stable during the moist cure, but after exposure to ambient conditions their shrinkage on drying showed the same relationship as the 7 day moist cure samples. Increasing the curing temperature to 60°C (140°F) and holding this temperature for 36 hours in a steam saturated environment, accelerated the hydration phase of the cure to 3 days (Cure 3). Steam curing improved moisture retention but more importantly shrinkage vs drying weight loss was reduced, as shown in Fig. 2. The improved stability with a change of cure conditions is an important result, but it will be difficult to accomplish this with job-site placed concrete.

Fig. 2 Drying Shrinkage vs. Weight Loss

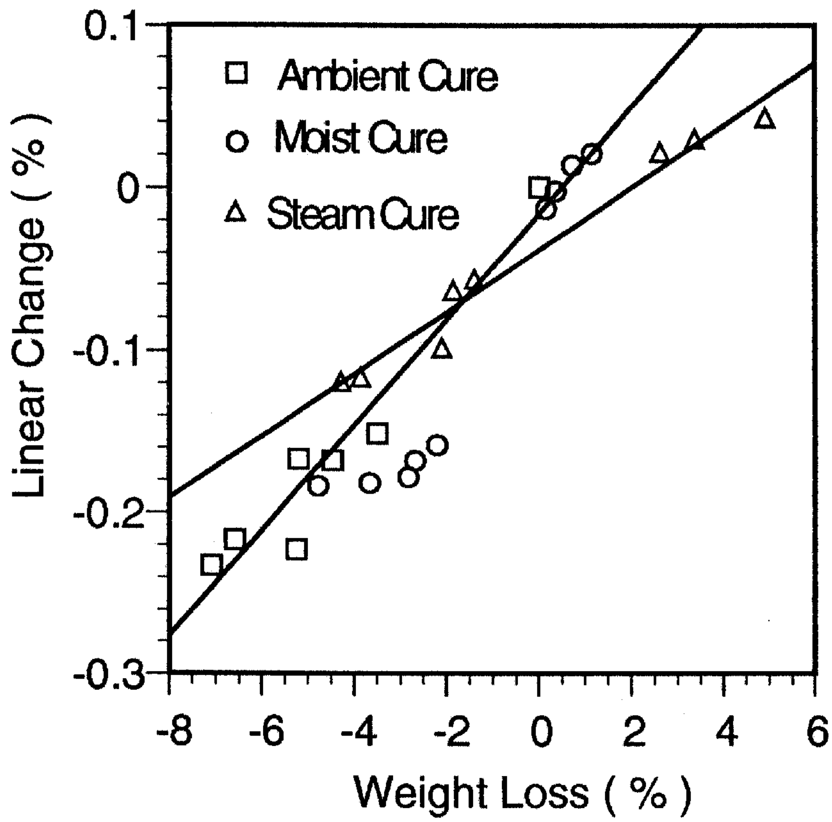

Fig. 2 Drying Shrinkage vs. Weight Loss

One potential way to steam cure the material without having to employ an on-site steam generator is to use the material's hydration exotherm to quickly bring the block to temperature. Because the material's filler is very light weight, its thermal mass is small and larger exotherms than normal are produced. By insulating the mold surfaces, the MBW50 material will exotherm and reach a temperature in excess of 200F in 12 to 18 hours as shown in Fig. 3. So long as the moisture is sealed in the material and temperature gradients are kept to a minimum (through insulation), it should experience sufficient time at temperature to get a thorough elevated temperature hydration. Initial experiments showed that acceptable mechanical properties could be obtained from this cure scheme and, while the shrinkage has not been measured, the surface quality indicates that the shrinkage is low. This type of autogenus cure will be examined more closely with larger scale specimens.

Fig. 3 Hydration Exotherm for MWB50

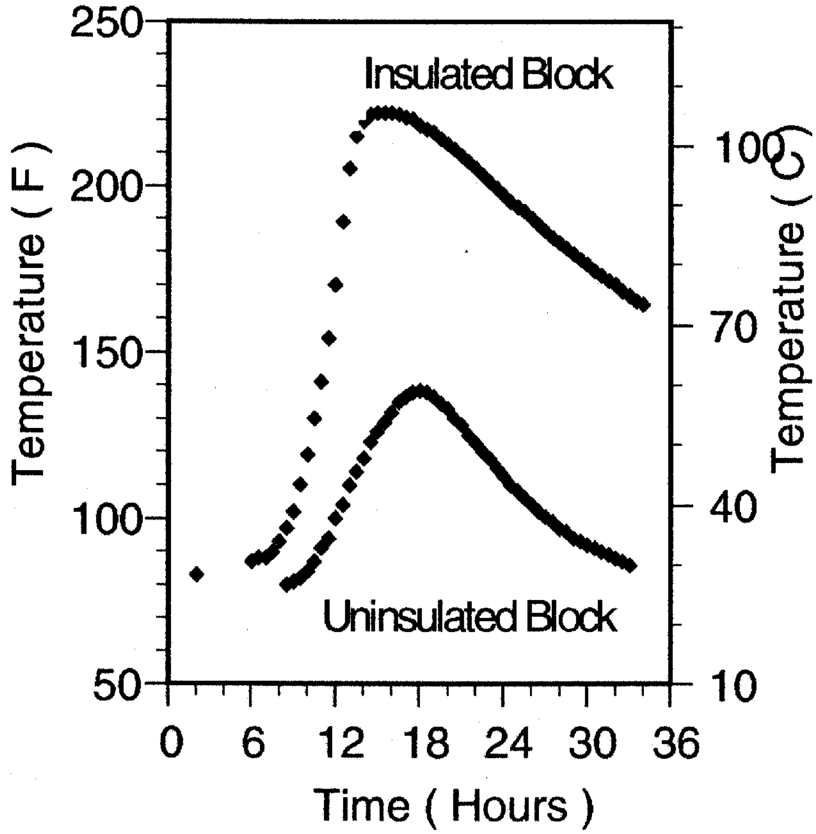

Fig. 3 Hydration Exotherm for MWB50

Mechanical Strengths

The mechanical testing showed a correlation between 28 days compressive strength and density. This strength/density relationship is illustrated in Fig. 4 for formulations that were mixed and cured under different conditions. The correlation is not surprising, since the reduction in density is related to the increase in porosity and the reduction in effective load-bearing area. Processing conditions must be carefully controlled to obtain consistant density and adequate strength. Weighing the quality control test cylinders when casting can be used as a quick means of checking the batch density and assuring future strength.

The splitting tensile strength was also plotted versus mix density as shown in Fig. 5. This property displayed a much weaker dependance on density than did the compressive strength.

Fig. 4. Compressive Strength of MBW50

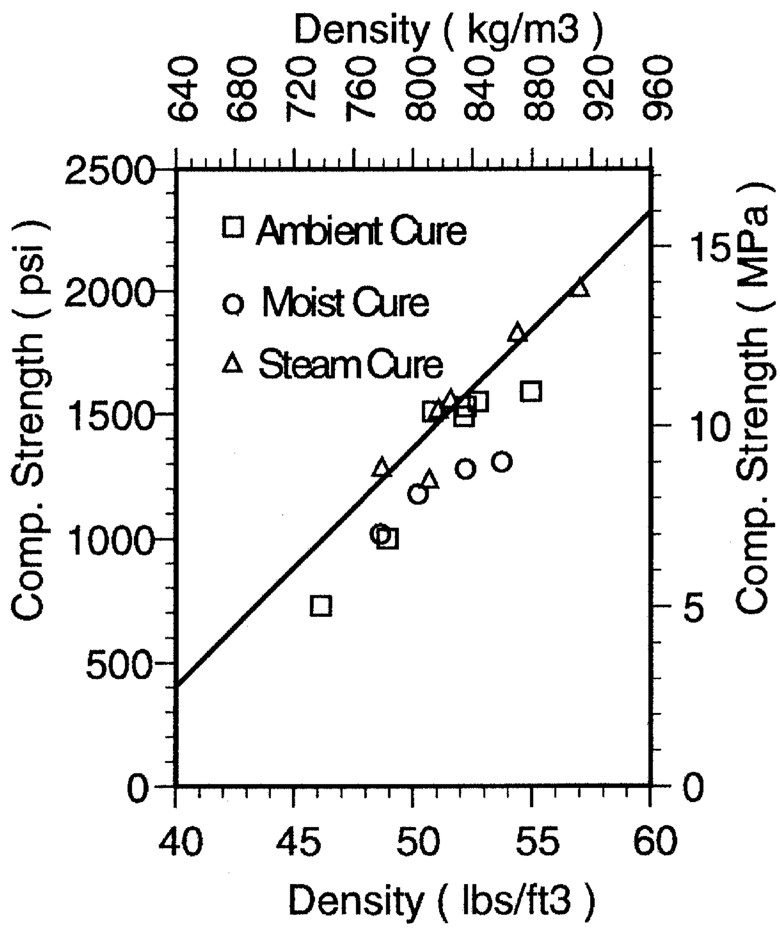

Fig. 4. Compressive Strength of MBW50

Fig. 5 Splitting Tensile Strength of MWB50

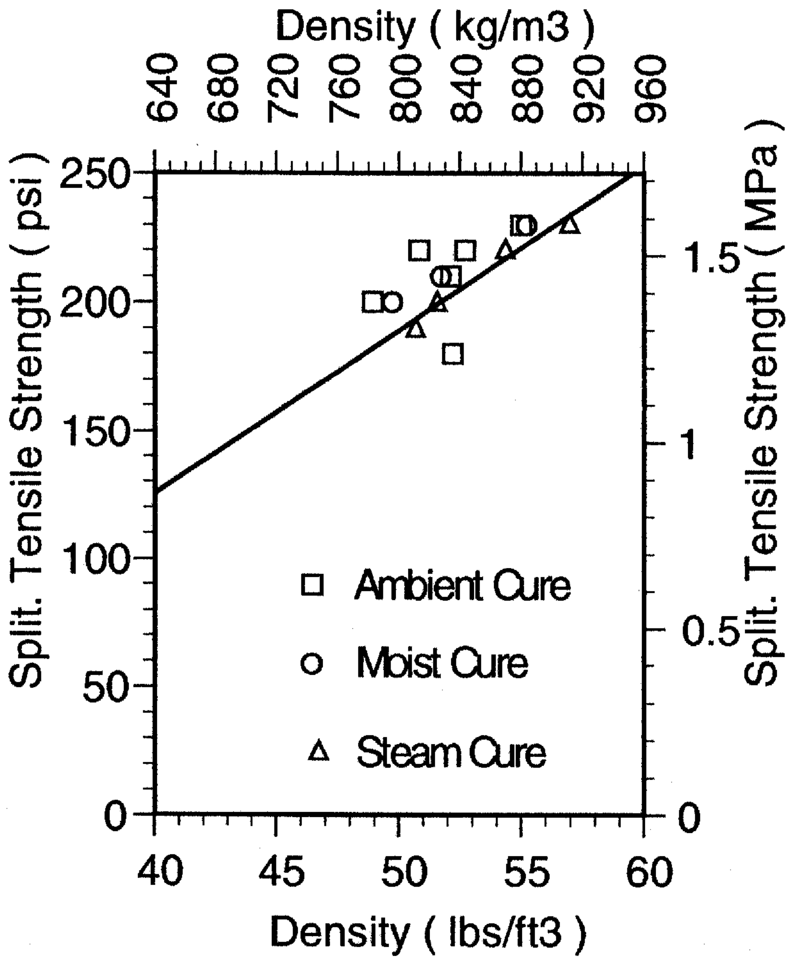

Fig. 5 Splitting Tensile Strength of MWB50

The mean mechanical strengths are summarized in Table II for the three cure conditions. The variation in compressive strength is partially due to the variation in density. But both small and large cylinders that were steam cured (cure 3) have higher compressive strengths at a given density than the ambient temperature cures (cures 1 &2). The flexure strengths measured were also highest after steam cure (350 psi), but as the beams dried the strengths dropped to 200 psi . The splitting tensile strengths reported showed no effect with cure.

Table II Mechanical Strengths of MWB50

	Cure 1	Cure 2	Cure 3
Comp. Strength (psi)	1420 +/- 240	1200 +/- 160	1630 +/- 330
Flex. Strength (psi)		275 +/- 35	270 +/-100
Split. Tensile Strength (psi)	220 +/- 20	210 +/- 20	210 +/- 30

Table II Mechanical Strengths of MWB50

Thermal Properties

The thermal properties were measured after moist curing. Heat capacity was determined by calorimetry, and thermal conductivity by the hot-wire method[5]. The heat capacity of the light weight material was found to be 1.3 kJ/kgK (0.31 Btu/lb) and the thermal conductivity was found to be 0.33 W/mK (2.2 Btu in/hrft^{2}F). Both the heat capacity and the thermal conductivity should be lower on drying. In the dilatometer[6] a pre-dried 1/4"x1/4"x1.5" sample heated from 30-130°C did not show consistent thermal expansion. Drying shrinkage due to the loss of absorbed moisture dominated. The changes were reversible due to swelling of the calcium silicate hydrate (C-S-H) gel with regained moisture on cool-down. So the sample was held in the dilatometer at 230°C to drive off the moisture, and the thermal expansion coefficient was measured between 230°C and 160°C on cool-down (above the temperature the sample could reabsorb ambient moisture).

3. Reinforced Concrete Tests

The new material was evaluated as a structural concrete in intermediate scale rebar reinforced beams and columns designed to the ACI Code. The structural elements were cast from three 500lbs mixes of MWB50, steam cured and tested after 28 days at CTL. The sample dimensions and rebar reinforcements are summarized in Table III. The preliminary results are summarized in the following tables.

Table III Intermediate Scale Structural Elements Reinforcing Schedule

	Sample #	Long. Reinforcement	Shear Reinforcement	Strain Gages
Flexural Beams	F1	(2) 6 mm Rebar	D2 Stirrups 3" Spacing	(2) on Rebar
(4"x8"x74")	F2	(3) 6 mm Rebar	D2 Stirrups 3" Spacing	(2) on Rebar
	F3	(4) 6 mm Rebar	D2 Stirrups 3" Spacing	(2) on Rebar
Shear Beams	S1 - S3	(4) 6 mm Rebar	None	None
(4"x8"x74")	S4 - S6	(4) 6 mm Rebar	D1 Stirrups 3" Spacing	(2) on Stirrups
Columns	C1	(8) #3 Rebar	#3 Ties 6" Spacing	(4) on Rebar
(8"x8"x72")	C2	(8) #4 Rebar	#3 Ties 8" Spacing	(4) on Rebar
	C3	(8) #5 Rebar	#3 Ties 8" Spacing	(4) on Rebar

Table III Intermediate Scale Structural Elements Reinforcing Schedule

Flexure Testing

The flexure specimens F1 to F3 were tested in 4-point bending over a 6 ft span. The number of 6 mm longitudinal reinforcement bars varied from 2 to 4 (the minimum and maximum allowed by the ACI Code requirements). The results are in Table IV.

The bending moment capacities M_b were calculated from $M_b = n A_s f_y (d - a/2)$. The tensile load on the longitudinal rebar is the product of the number of rebar n, the rebar cross-sectional area A_s, and the steel yield strength f_y (60ksi). The moment arm is (d - a/2) where d is distance from the top face to the rebar centroid and the depth of the compression zone a is given by $a = A_s f_y / 0.85 f_c b$. The compressive strength of the concrete f_c was taken as 1500 psi and b is the beam width.

Table IV Flexure Beam Test Results

#	Max. Applied Moment (ft-kip)	Calc. Moment Capacity (ft-kip)	%
F1	4.25	3.46	123
F2	6.04	4.96	122
F3	6.14	6.32	97

Table IV Flexure Beam Test Results

The flexural cracking in beams F1, F2 and F3 was uniformly distributed along the length of the members, indicating that there was adequate bond between the reinforcing steel and the lightweight concrete. All of the members except F3 exceeded their calculated capacities. F3 exhibited a compression failure below one of the loading plates at the top of the beam.

Shear Testing

The shear specimens were tested in 4-point bending over a reduced 4 ft span. The upper loading rollers were 1 ft apart. S1-S3 contained 4 longitudinal 6mm rebar, but no shear reinforcement. S4-S6 were reinforced with shear stirrups at 3" spacings (the maximum spacing allowed by ACI). The results are summarized in Table V.

The total shear capacity V is the sum of the shear capacity V_c of the concrete and the load capacity of added stirrup reinforcements V_s.

The capacity of beams without stirrups is $V_c=2\ b\ d(f_{ct}/6.7)$ where f_{ct} is the cylinder splitting tensile strength (200 psi) and b and d are defined as above. The increased capacity when adding stirrups is $V_s=A_v\ f_y\ d/s$ where A_v is the area of the stirrup(2x) and s is the stirrup spacing.

Table V Shear Beam Test Results

#	Max. Applied Shear (kip)	Calc. Shear Capacity (kip)	%
S1-3	1.93 +/- 0.13	1.74	121
S4-6	4.46 +/- 0.56	3.74	119

Table V Shear Beam Test Results

The shear beams showed flexure cracks on initial loading, but all the failures were due to long diagonal shear cracks for both the shear unreinforced and lightly shear reinforced beams (compared to the flexure beams).

Column Testing

The column specimens were loaded in uniaxial compression. The longitudinal rebar reinforcements for columns C1, C2 and C3 covered 1.4%, 2.5% and 3.9% of the loaded cross-sectional area. The columns were also reinforced with transverse ties. The results are summarized in Table VI.

The axial load capacity of the columns P_c is the sum of the load capacities of the concrete and steel. $P_c = 0.8\ (0.85\ f_y\ A_c + f_y\ A_s)$ where A_c is the concrete cross-sectional area and the other parameters are as previously defined.

Table VI Column Test Results

#	Max. Applied Axial Load (kip)	Calc. Axial Load Capacity (kip)	%
C1	126.2	106.6	118
C2	189.6	140.4	135
C3	252.8	181.8	139

Table VI Column Test Results

All of the rebar reinforced members (flexure beams, shear beams or columns) exhibited ductile behaviour at failure. None of the members failed suddenly, without warning, a desirable characteristic in structural applications.

Small Gage Mesh Reinforcements

Standard heavy rebar reinforcements would not be advisable for use in the non-propagating walls of the HPM magazine, due to the risk of impact on acceptor munitions in the case of an accident. Welded wire mesh and expanded metal mesh reinforcements should avoid this hazard, so they were evaluated on smaller beams. The meshes were bent and extended up the sides of the beam as an open cage to provide shear reinforcement as well. The reinforcement schedule is listed in Table VII.

Table VII 4"x6"x36" Mesh Reinforced Beams

Sample #	Reinforcements
M1-2	3/4" 16 gage exp. metal sheet
M3-4	1.5" 16 gage exp. metal sheet
M5-6	1x2" 14 gage rect. welded wire
M7-8	2x4" 14 gage rect. welded wire

Table VII 4"x6"x36" Mesh Reinforced Beams

The beams were tested in 3-point loading. The bending moments are summarized in Table VIII. The load-deflection curves for the mesh reinforced samples are illustrated in Fig. 6. The smaller rectangular wire mesh reinforcement appears to be as effective as the expanded metal meshes. The larger wire mesh was less effective due to the reduced number of wires.

Table VIII 3-Point Bending Results

#	Max. Bending Moment (ft-kip)	Failure
M1-2	1.50-1.52	Ductile
M3-4	1.31-1.46	Ductile
M5-6	1.55-1.60	Ductile
M7-8	0.88-0.92	Ductile

Table VIII 3-Point Bending Results

Fig. 6 Mesh Reinforced Beams

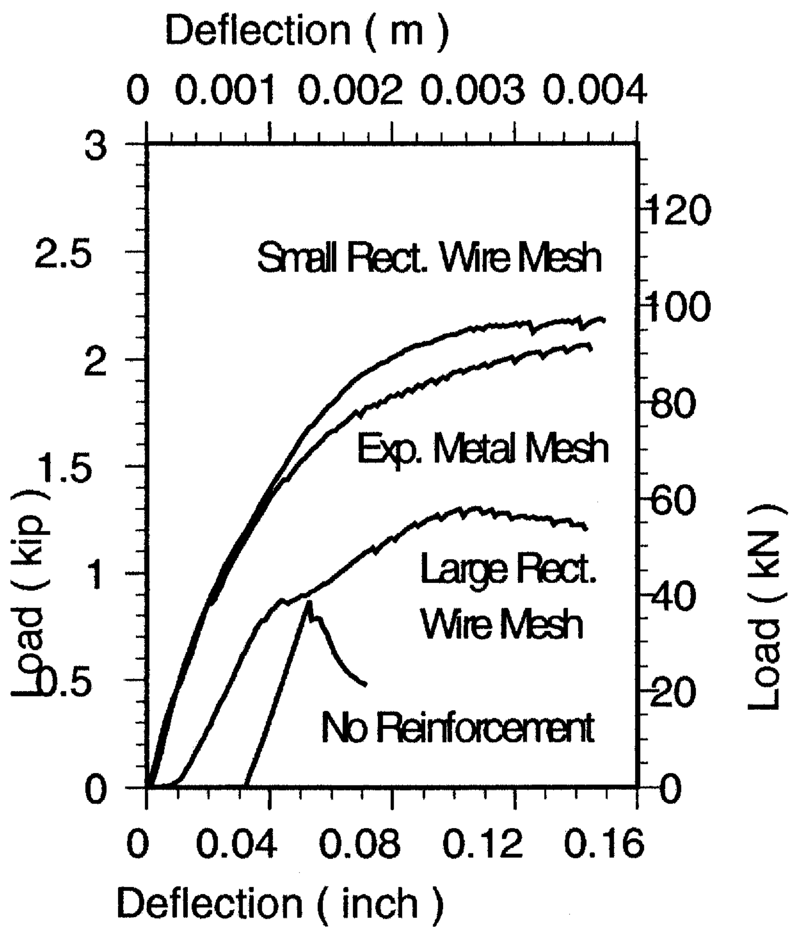

Fig. 6 Mesh Reinforced Beams

Bond Development vs. Cure

Reinforced structural concrete must develop a good bond between the reinforcement and the concrete in order to obtain the full composite properties. As part of the cure development scheme, 6mm, #3 and #4 rebar were cast in 4"x8"cylinders for pullout tests. In Table IX the rebar pullout strengths are listed for the different bar sizes and cure conditions.

Table IX Rebar Pullout Strengths vs. Cure

	Cure 1	Cure 2	Cure 3
De-Bond Strength (psi)			
6 mm Rebar	110 +/- 90		490 +/- 60
#3 Rebar	470	410	480
#4 Rebar	140	410	440
Max. Pullout Strength (psi)			
6 mm Rebar	160 +/- 100		460 +/- 150
#3 Rebar	410	330	380
#4 Rebar	260	390	420

Table IX Rebar Pullout Strengths vs. Cure

The pullout load-displacement curves showed a sharp initial debonding peak and then a broader second peak due to the mechanical keying of the rebar grooves. The average bond strength is about 400 psi. Ambient cure 1 had a high proportion of poorly bonded samples, where drying shrinkage may have weakened the bonding, or cracks could reduce the effective bond length under load. The pullout strengths were improved by the steam cure 3 due to better bond development.

4. SUMMARY AND CONCLUSIONS

Finally, the properties for the new material MWB50 are summarized and listed with the earlier GC-2 material in Table X for comparisons.

Table X Lightweight Concrete Materials

SA/CBC Materials	Units	GC-2	MWB50
Density	**kg/m^3**	**550**	**800-870**
	lbs/ft^3	35	50-54
Porosity	**%**	**75**	**60**
Compressive Strength	**MPa**	**8.3**	**10.3**
	psi	1200	1500
Split. Tensile Strength	**MPa**	**0.7**	**1.4**
	psi	100	200
Flexure Strength	**MPa**		**1.4**
	psi		200
Rebar Bond Strength	**MPa**		**2.7**
	psi		400
Elastic Modulus	**GPa**	**1.7**	**3.4**
	10^6 psi	0.25	0.5
Shrinkage	**%**	**0.22**	**0.10**
	in/in	0.0022	0.0010
Heat Capacity (moist)	**kJ/kgK**		**1.3**
	btu/lb^{o}F		0.31
Thermal Conductivity (moist)	**W/mK**		**0.33**
	$\frac{\text{btu in}}{\text{hr ft}^2 {}^o\text{F}}$		2.2
Coefficient of Thermal Expansion (160-230^{o}C)	**$10^{-6}/^oC$**		**5.1**
(320-450^{o}F)	$10^{-6}/^oF$		2.9
Materials Costs	**$/m^3**	**920**	**200**
	$/yd^3	700	160

Table X Lightweight Concrete Materials

The new material MWB50 achieves the desired mechanical properties with a cost-effective formulation. The material may be placed in the field using standard construction practices so long as precautions are taken to control the cure.

The structural characterization confirms it behaves in accordance with ACI design codes in common intermediate scale elements. The material bonds well to steel surfaces, if the shrinkage is controlled. Small gage mesh materials may be very efficient as reinforcements. The dimensional stability is marginal. The rate of moisture loss is higher than desirable due to the permeability of the intrinsically porous material. The stability can be improved with elevated temperature curing either by using steam or by controlling the hydration exotherm duration. The latter can be managed by a combination of adjusting cement reactivity and insulating the casting forms used.

The material is non-flammable and highly permeable, so there is no risk of explosive spalling on heating. But the material properties should degrade with higher temperature exposure.

Future work will look at the longer term stabilty of the material. Creep and freeze-thaw tests are in progress. The dimensional stability needs improvement and can be further optimized through control of the cure condition. The material batch size will be scaled up in larger processing equipment. The shock-absorption characteristics should be determined from flyer plate impact tests to establish the Hugoniot curve for the material. Sympathetic detonation tests with live acceptors will be carried out for the HPM magazine early next year.

Acknowledgements

The authors wish to thank the Naval Facilities Engineering Service Center in Port Hueneme, CA for their financial and technical support under SBIR Contract N47408-93-C-7357 titled "Development of Structural Shock Absorbing Cement Based Materials for Magazine Construction", Jim Tancreto COTR. In addition the authors thank Gene Corley, Tim Dickson and Ron Berg of Construction Technology Laboratories for their technical support in design and testing of the reinforced structural elements of MWB50.

References

1. C39-86 "Test Method for Compressive Strength of Cylin-drical Concrete Specimens", ASTM Vol. 04.02 (1993)

2. C496-90 "Test Method for Splitting Tensile Strength of Cylindrical Concrete Specimens", 04.02 (1993)

3. C348-93 "Test Method for Flexural Strength of Hydraulic Cement Mortars " ASTM Vol.   04.01 (1993)

4. C490-93a "Use of Apparatus for the Determination of Length Change of Hardened Cement Paste, Mortar, and Concrete", ASTM 04.01 (1993)

5. "Thermal Transmission Measurements of Insulation, ASTM STP 660, R.P. Tye, Ed., 1978 pp 147-199

6. E372-81 "Linear Thermal Expansion of Rigid Solids with a Vitreous Silica Dilatometer"   ASTM Part 17 (1982)